

# Study of the Conformational Profile of the Norbornane Analogues of Phenylalanine

ARNAU CORDOMÍ,<sup>a</sup> JESUS GOMEZ-CATALAN,<sup>a,b</sup> ANA I. JIMENEZ,<sup>c</sup> CARLOS CATIVIELA<sup>c</sup> and JUAN J. PEREZ<sup>a\*</sup>

<sup>a</sup> Dept. d'Enginyeria Quimica, UPC, ETSEIB, Av. Diagonal, 647; 08028 Barcelona, Spain

<sup>b</sup> Dept. de Toxicologia, Facultat de Farmacia, Universitat de Barcelona, Av. Joan XXIII, s/n; 08028 Barcelona, Spain

<sup>c</sup> Dept. de Quimica Organica, Instituto de Ciencia de Materiales de Aragon, Universidad de Zaragoza, CSIC, 50009 Zaragoza, Spain

Received 2 January 2002

Accepted 5 February 2002

**Abstract:** The conformational profile of the eight stereoisomeric 2-amino-3-phenylnorbornane-2-carboxylic acids (2-amino-3-phenylbicyclo[2.2.1]heptane-2-carboxylic acids) has been assessed by computational methods. These molecules constitute a series of four enantiomeric pairs that can be considered as rigid analogues of either L- or D-phenylalanine. The conformational space of their N-acetyl methylamide derivatives has been explored within the molecular mechanics framework, using the parm94 set of parameters of the AMBER force field. Local minimum energy conformations have been further investigated at the *ab initio* level by means of the Hartree-Fock and second order Moller-Plesset perturbation energy calculations using a 6-31G(d) basis set.

The results of the present work suggest that the bulky norbornane structure induces two kinds of conformational constraints on the residues. On one hand, those of a steric nature directly imposed by the bicycle on the peptide backbone and, on the other hand, those that limit the orientations attainable by the phenyl ring which, in turn, reduces further the flexibility of the peptide backbone. A comparative analysis of the conformational profile of the phenylnorbornane amino acids with that of the norbornane amino acids devoid of the  $\beta$ -phenyl substituent suggests that the norbornane system hampers the residue to adopt extended conformations in favour of C7-like structures. However, the bicycle itself does not impart a clear preference for any of the two possible C7 minima. It is the aromatic side chain, which is forced to adopt an almost eclipsed orientation, that breaks this symmetry introducing a marked preference for a single region of the ( $\phi$ ,  $\psi$ ) conformational space in each of the phenylalanine norbornane analogues investigated. Copyright © 2002 European Peptide Society and John Wiley & Sons, Ltd.

**Keywords:** phenylalanine analogues; constrained amino acids; bicyclic amino acids; norbornane; conformational study; AMBER

## INTRODUCTION

Unnatural amino acids are useful tools in the fields of peptide design, the study of the conformational

profile of peptides, synthesis of bioactive peptide analogues with improved pharmacokinetic properties, development of pharmacophore models and protein engineering [1–5]. They are basically designed by structural transformation of natural amino acids and, depending on the changes introduced, the new compounds may exhibit conformational profiles completely different to those of their natural counterparts. This offers the

\*Correspondence to: Dr Juan J. Perez, Department d'Enginyeria Quimica, UPC, ETSEIB, Av. Diagonal, 647, 08028 Barcelona, Spain.

Contract/grant sponsor: DGES.

Contract/grant sponsor: DGA; Contract/grant number: PM98-0012-C02-01; PPQ2001-1834 and P22-98.

opportunity to identify new amino acids that can play a role as inducers of structural preferences in peptide analogues. These features are especially relevant in the case of aromatic residues, since their side chains have been implicated in many examples of ligand-receptor recognition, as well as in protein-DNA contacts [5–7]. Furthermore, aromatic-aromatic  $\pi$ -stacking [8] and  $\pi$ -hydrogen bond [9,10] interactions have been implicated as important factors in the stabilization of the tertiary structure of proteins.

In the framework of a long-term project devoted to understanding the conformational features induced by different phenylalanine derivatives, we have previously reported computational studies on the conformational analysis of some analogues incorporating an additional methyl and/or phenyl group at the  $\alpha$  and/or  $\beta$  position [11]. In the same direction, we have also reported theoretical [12,13] and experimental [13–16] results on the structural behaviour of cyclic phenylalanine surrogates in which the  $\alpha$  and  $\beta$  carbons are included in a three- or six-member ring (denoted as  $c_3$ Phe and  $c_6$ Phe, respectively, in Figure 1). In the open-chain analogues studied, the additional substituents reduce the flexibility of the backbone but the mobility of the side chain is only slightly limited. In contrast, in the cyclic derivatives investigated the structural modifications impart severe restrictions to the orientations attainable by the aromatic side chain, and have proven very efficient in the induction of specific structural motifs to the peptide backbone.

The focus of the present work was to establish the conformational profile of the norbornane analogues of phenylalanine (2-amino-3-phenylnorbornane-2-carboxylic acids, Figure 1) in order to assess their

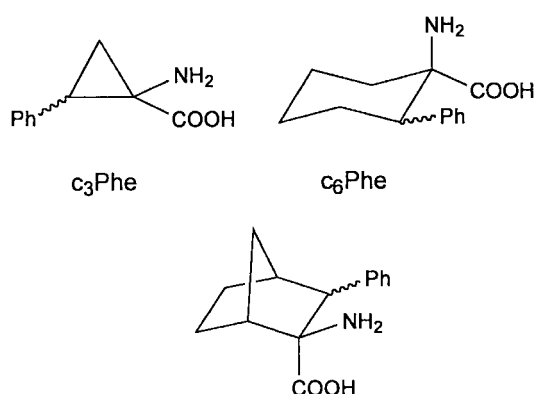


Figure 1 Structure of different constrained analogues of phenylalanine. The norbornane surrogates (below) are investigated in the present study.

potential use as building blocks in the design of constrained peptide analogues. Interest in the biological properties of amino acids containing a norbornane skeleton is not new. They can improve the resistance of peptides to enzymatic hydrolysis (a major drawback in the application of peptides as therapeutic drugs) and have shown noticeable specific biological behaviour in some cell membrane transport systems [17,18]. This latter property may be of high value in the preparation of peptide surrogates with improved bioavailability. Interest in the norbornane analogues of phenylalanine has stimulated the development of synthetic methods to prepare them [19–21].

Cyclization modifies the conformational profile of amino acids in several ways: (1) reduces the asymmetry of the  $C^\alpha$  carbon, breaking the right handed preference of the secondary structure exhibited by L-amino acids; (2) introduces additional steric hindrance, especially in the extended conformations of the peptide chain; (3) ring closure limits the orientations attained by the rest of the side chain moieties, thus favouring certain values for the  $\chi^1$  dihedral angle, that can be different from those preferentially adopted by their linear counterparts; (4) indirectly, restrictions on  $\chi^1$  may induce some constraints on the  $(\phi, \psi)$  conformational space [22].

These effects arising from cyclization have been analysed in detail for the aforementioned phenylalanine cyclopropane ( $c_3$ Phe) and cyclohexane ( $c_6$ Phe) analogues [12–16]. In the norbornane derivatives selected for the present study, the  $\alpha$  and  $\beta$  carbons are included in a cyclohexane ring, as occurs in  $c_6$ Phe. The additional methylene bridge in the norbornane skeleton does, however, introduce important stereo structural differences between the two systems. Besides the extra steric hindrance, the presence of the methylene group forces the cyclohexane ring to adopt a boat-like structure, whereas in  $c_6$ Phe the six-member cycle is free to accommodate the more favoured chair disposition [13]. Concomitantly, in the rigid norbornane derivatives, the phenyl ring is fixed at  $\chi^1$  dihedral values close to  $0^\circ$  or  $\pm 120^\circ$  depending on the configuration of the  $\alpha$  and  $\beta$  carbons. These dihedrals correspond to eclipsed orientations, in contrast to the staggered side chain arrangements that characterize the  $c_6$ Phe derivatives and phenylalanine [13]. As far as the side chain conformation is concerned, the norbornane analogues of phenylalanine are structurally similar to  $c_3$ Phe, given that the cyclopropane moiety also confines the aromatic substituent to eclipsed orientations.

The bicyclic system also has implications with regard to the number of isomeric forms available. Whereas four different stereoisomers are possible for both  $c_3$ Phe and  $c_6$ Phe, the phenylalanine norbornane surrogates exhibit the eight isomeric structures illustrated in Figure 2 (four chiral centres are present, but configurations of C1 and C4 are actually interdependent). They correspond to analogues of L- or D-phenylalanine, as defined by the stereochemistry at C $^\alpha$ .

A computational study was performed, at the molecular and quantum mechanics levels, on the four stereoisomers that formally derive from L-phenylalanine. However, the results can be extended to the D-phenylalanine analogues because the Ramachandran maps of two enantiomers are symmetry related so that a point ( $\phi, \psi$ ) on the map of a compound corresponds to the point ( $-\phi, -\psi$ ) of its enantiomer. Thus, for example, the map of the (2R) *cis-endo* stereoisomer can be obtained from that computed for the (2S) *cis-endo* derivative by simply changing the sign of both dihedrals. We have also studied the conformational profile of the parent norbornane amino acids, which do not have the aromatic substituent, with the aim of differentiating direct constraining effects induced by the norbornane skeleton from those arising from the reduction of the phenyl side chain flexibility.

## METHODS

Conformational analysis was performed on the N-acetyl methylamide derivatives of the different amino acids (Ac-Xaa-NHMe, dipeptides) in order to mimic the progression of the peptide chain. Conformational energies were computed within the molecular mechanics framework using the parm94 parameterization of the AMBER force field [23]. Although this set of parameters reproduces with acceptable accuracy the conformational features of natural amino acids, in order to check the quality of the description obtained on the different bicyclic derivatives, whole geometry *ab initio* optimizations at the Hartree-Fock level using a 6-31G(d) basis set were carried out on each of the local minima previously located at the molecular mechanics level. Furthermore, in order to assess the relative energy of the different minima the energy was also evaluated using the Moller-Plesset perturbation theory up to second order using the geometries optimized in the Hartree-Fock calculations. All these calculations were performed with the Gaussian94 package [24].

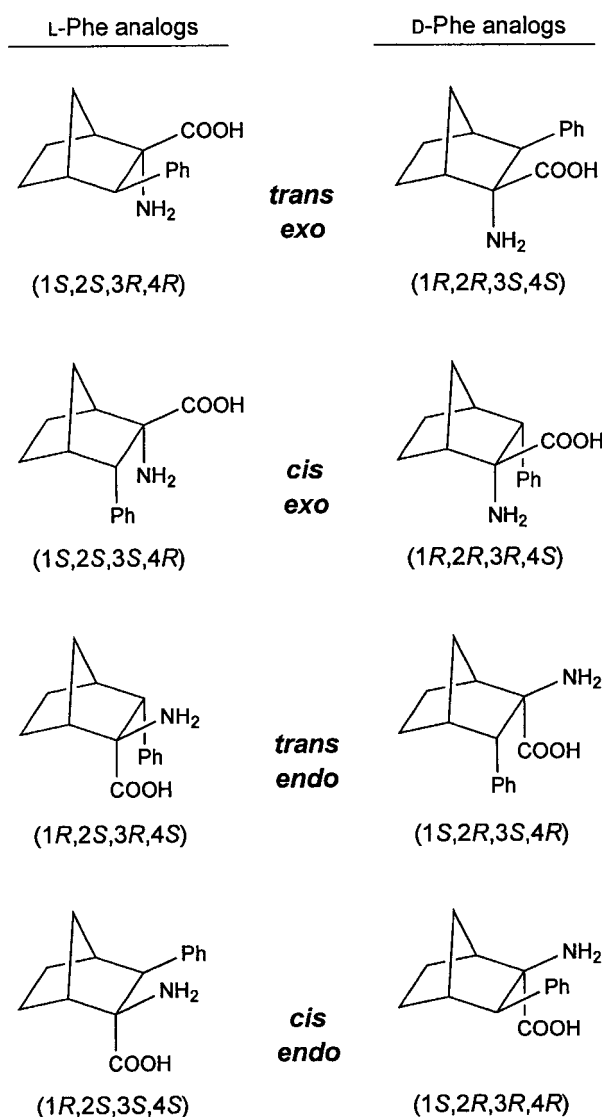


Figure 2 Structure of the eight stereoisomeric norbornane analogues of phenylalanine. The left column shows pictorially the four L-phenylalanine derivatives (S configuration at the  $\alpha$  carbon), and their respective enantiomers (derived from D-phenylalanine) are depicted in the right-hand side column. *Cis* and *trans* are defined by the relative disposition of the phenyl and amino substituents. The *exo/endo* stereochemistry is marked by the orientation of the carboxyl moiety with respect to the bicyclic structure: in the *exo* derivatives the carboxyl function is closer to the methylene bridge. Positions 1 and 4 correspond to the bridgehead atoms, while the  $\alpha$  and  $\beta$  carbons occupy positions 2 and 3, respectively.

For the selection of the basis set previous experience was taken into account suggesting that this basis set provides accurate results for this kind of study [25–27].

For each of the residues studied in the present work the following steps were performed: (1) construction of the dipeptide molecule in the all-*trans* conformation; (2) computation of a set of RESP atomic charges by fitting the molecular electrostatic potential computed at the Hartree-Fock level with a 6-31G(d) basis set; (3) computation of the Ramachandran plots *in vacuo* using a 10° grid; energy was computed with the parm94 set of parameters of the AMBER force field by freezing the values of  $\phi$  and  $\psi$  and allowing full optimization of the rest of the geometry; (4) complete energy optimization was carried out on each of the local minima evidenced on the Ramachandran plots, both by molecular and quantum mechanics methods; (5) additionally, other possible minima associated to alternative values of the  $\chi^2$  dihedral, defining the orientation of the phenyl plane, were investigated; (6) local minima were used as starting points for the *ab initio* calculations.

## RESULTS AND DISCUSSION

The Ramachandran maps of the four L-phenylalanine norbornane analogues computed within the molecular mechanics framework are shown in Figure 3. Local minima are denoted by crosses on the maps. Relative conformational energies, referred to as the respective global minimum, as well as the values of the  $\phi$ ,  $\psi$ ,  $\chi^1$  and  $\chi^2$  dihedrals of the identified local minima, computed with both molecular mechanics and *ab initio* methods, are listed in Table 1.

Maps of the parent norbornane amino acids are shown in Figure 4. Values of the  $\phi$ ,  $\psi$  dihedrals and relative energies for the local minima identified are listed in Table 2.

Three main aspects regarding these results are discussed in the present section. The first concerns the assessment of the quality of the results, as judged by the consistency between the molecular and the quantum mechanics values obtained. The second is devoted to analysing the main features observed in the conformational profiles of the residues on the basis of their different structural origins. Finally, the possible implications of using these residues in peptide design are considered.

The results listed in Table 1 suggest that there is a solid consistency between the geometry of the minima obtained using the AMBER force field and those computed at the *ab initio* level, even if 3 of the 22 minima characterized at the

molecular mechanics level are not minima in the quantum mechanics computations. Average values of the absolute differences between the two sets of calculations are small, being 9°, 18°, 5° and 7° for dihedrals  $\phi$ ,  $\psi$ ,  $\chi^1$  and  $\chi^2$ , respectively. The larger deviation exhibited by the  $\psi$  dihedral is mainly due to one of the minima found for the *cis-exo* stereoisomer (minimum **E**), for which the molecular mechanics calculation predicts a conformation with  $\psi$  close to 0°, whereas the *ab initio* calculations predict a helical structure with  $\psi$  near 50°. However, this is a secondary minimum with a relative energy of about 6 kcal/mol above the global minimum and is difficult to access.

For each of the phenylalanine analogues studied, both computational methods agree on the prediction of the absolute minimum. The consistency of the relative energy of the secondary minima is also quite acceptable, with the average of the absolute deviations between molecular and quantum mechanics calculations at the MP2 level being 1.5 kcal/mol. The relative ordering of the different minima for each residue is also consistent, with the exception of conformation **D** of the *trans-endo* isomer, that is predicted to be the first excited state in the quantum mechanics calculations, at only 2.6 kcal/mol above the global minimum, whereas it is minimum #7 according to the AMBER results, at 6.3 kcal/mol above the global minimum. This conformation is characterized by a close contact between the acetyl oxygen atom and two hydrogens of the bicycle skeleton (Figure 5). The discrepancy between the two results may be due to the difference in the evaluation of this repulsive interaction. In fact, the distance between the oxygen atom and the skeleton hydrogens is larger in the molecular mechanics than in the quantum mechanics geometry (Figure 5), suggesting an overestimation of the repulsion energy in the molecular mechanics calculation that, consequently, induces a larger distortion in the amide bond angle. Moreover, the N – C $^\alpha$  – C' angle ( $\tau$ ) computed at the molecular mechanics level is 105°, while the value computed at the quantum mechanics level is only 102°, considerably more closed than the standard equilibrium AMBER value (110.1°). It is possible that AMBER overestimates the bending energy that permits the alleviation of the hindrance with the norbornane skeleton. In order to assess whether this discrepancy is maintained in the absence of the phenyl moiety these results were compared with those obtained for the unsubstituted *endo* norbornane amino acid. Table 2 shows that the relative energy of conformation **D** is almost 3 kcal/mol lower

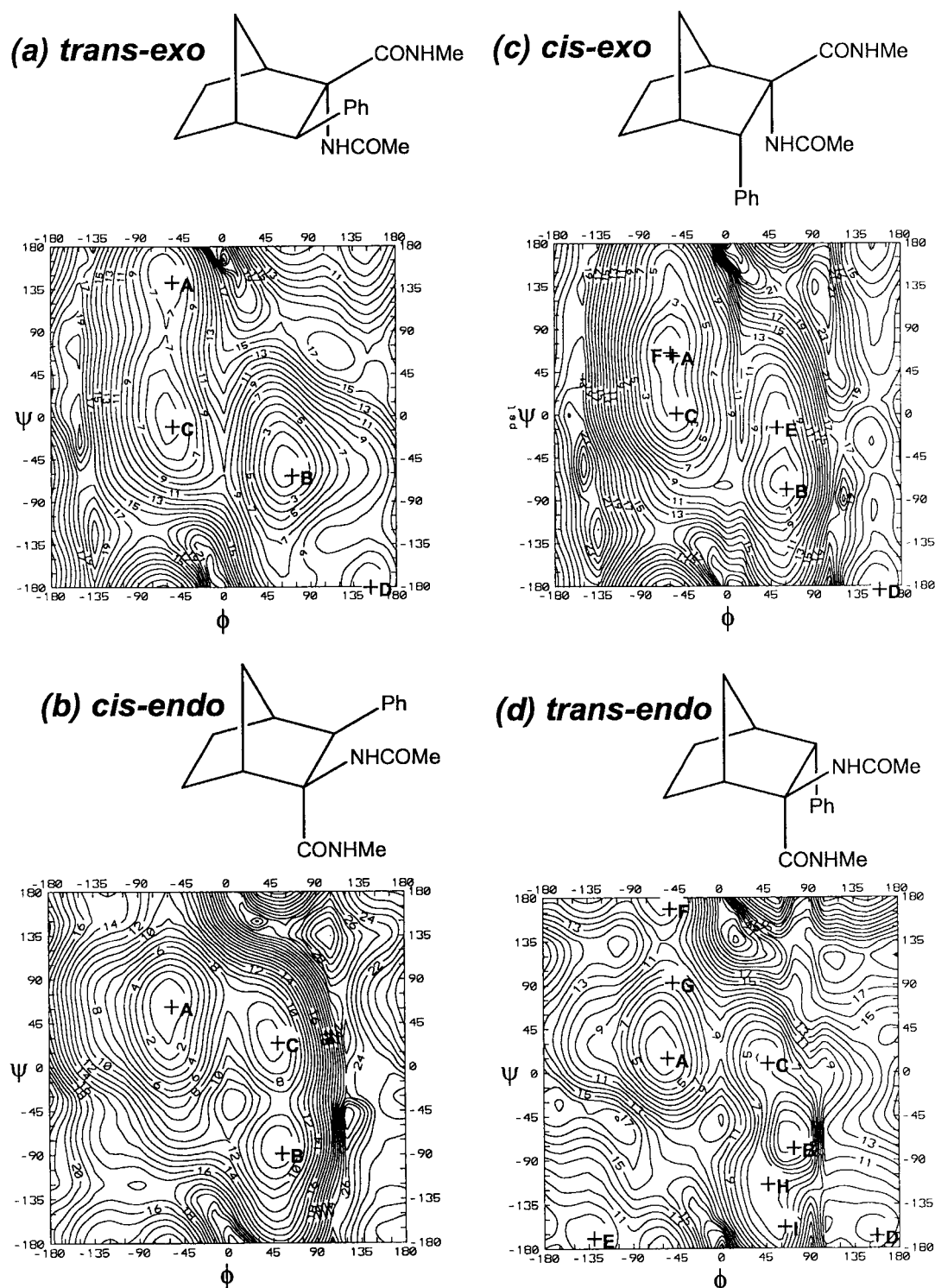


Figure 3 Structures and Ramachandran maps of the dipeptides Ac-Xaa-NHMe, where Xaa represents each of the four stereoisomeric norbornane analogues of L-phenylalanine. Contour lines represent AMBER relative energy and are drawn at intervals of 1.0 kcal/mol. Low-energy conformations are located on the map with crosses and labelled with letters. See Table 1 for a description of their geometries and energies. (a) *trans-exo* isomer; (b) *cis-endo* isomer; (c) *cis-exo* isomer; (d) *trans-endo* isomer.

Table 1 Relative Energy (kcal/mol) and Dihedrals (degrees) of the AMBER and *ab initio* Minima Characterized for the Phenylnorbornane Dipeptides Represented in Figure 3

	AMBER					HF/6-31G*					MP2/6-31G*
	E(kcal/mol)	$\phi$	$\psi$	$\chi^1$	$\chi^2$	E(kcal/mol)	$\phi$	$\psi$	$\chi^1$	$\chi^2$	E(kcal/mol)
<i>trans-exo</i>											
A	5.87	-60	151	116	105	2.92	-61	147	113	98	4.46
B	0.00	65	-55	112	79	0.00	79	-51	113	71	0.00
C	4.31	-59	-1	112	117	1.88	-67	-32	105	79	3.11
D	6.89	149	-176	112	109	5.64	160	-158	103	114	4.61
<i>cis-endo</i>											
A	0.00	-61	69	19	99	0.00	-76	67	19	96	0.00
B	6.89	50	-82	25	85	8.06	50	-112	21	71	8.05
C	5.40	45	27	20	100	4.95	49	49	15	94	4.52
<i>cis-exo</i>											
A	0.00	-62	70	22	53	0.00	-76	67	20	59	0.00
B	4.29	56	-72	16	124	6.61	62	-88	7	133	6.13
C	0.40	-59	15	25	54	(a)					
D	11.81	151	180	23	51	13.84	160	-158	18	52	12.83
E	4.58	44	-2	30	62	6.79	39	53	21	62	6.91
F	2.31	-65	72	15	117	0.93	-79	65	10	120	1.36
<i>trans-endo</i>											
A	1.84	-60	19	105	51	2.86	-75	38	100	50	2.86
B	0.00	67	-67	120	126	0.00	79	-63	123	135	0.00
C	3.00	51	2	117	48	5.09	62	30	113	47	5.27
D	6.28	152	-161	104	52	3.48	170	-146	96	54	2.63
E	7.91	-135	-167	101	52	(b)					
F	8.07	-61	178	110	52	6.77	-63	-178	109	49	7.00
G	5.98	-56	99	120	134	3.99	-59	118	120	140	4.66
H	4.68	43	-106	105	68	3.65	50	-144	113	54	3.86
I	5.20	63	-160	118	44	(c)					

<sup>a</sup> Minimization leads to minimum A.

<sup>b</sup> Minimization leads to minimum D.

<sup>c</sup> Minimization leads to minimum H.

at the *ab initio* level, suggesting that a similar effect is produced. This indicates that the molecular mechanics computations do not reproduce accurately the quantum mechanics energy profile in this region of the Ramachandran plot of the *endo* norbornane amino acids. However, and because of the acceptable consistency of the rest of minima and the lack of experimental data, we considered that it was not worth at this stage developing new molecular mechanics parameters.

The main features of the conformational profiles of the phenylnorbornane amino acids can be understood by comparison with those of their unsubstituted counterparts. Therefore, we begin this section by analysing the maps in Figure 4.

The map of the *exo* isomer (Figure 4a) is characterized by a quite symmetric profile, with

two main minima that are almost isoenergetic and correspond to C7 structures. These low-energy regions are wide in the  $\psi$  component and narrow along the  $\phi$  axis, suggesting a stronger restriction on the rotation about the C $\alpha$ –N angle. The map of the *endo* isomer (Figure 4b) is more complex. The two most important minima are also C7 conformations. However, the valley of minimum **B** splits into two different structures and, in the region of minimum **A**, the slope of the energy surface is not as steep as the corresponding minimum of the *exo* isomer along the  $\phi$  axis. In contrast, the  $\psi$  dihedral appears more restricted in the map of the *endo* isomer (Figure 4b) and (Figure 4a). For both the *exo* and the *endo* residues, extended conformations of the C5 type are highly destabilized.

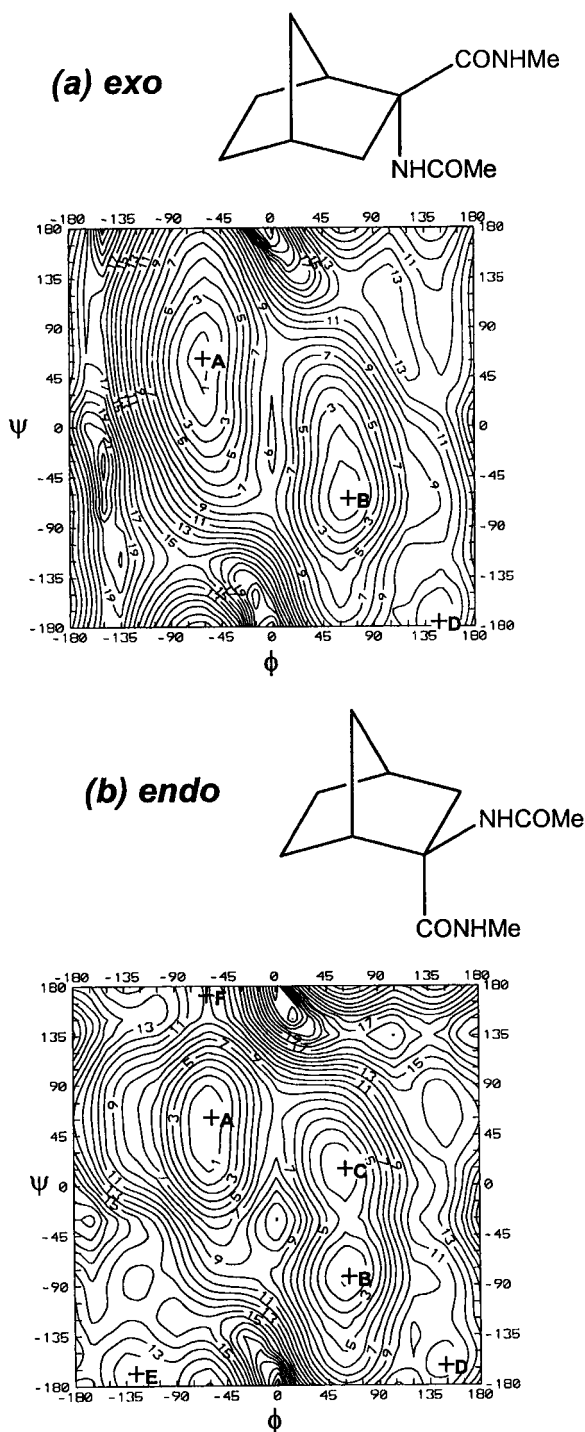


Figure 4 Structures and Ramachandran maps of the dipeptides Ac-Xaa-NHMe, where Xaa represents *exo*- and *endo*-2-aminonorbomane-2-carboxylic acids. Contour lines represent AMBER relative energy and are plotted every kcal/mol. Low-energy conformations are located on the map with crosses and labelled with letters. Their geometries and energies are given in Table 2. (a) *exo* isomer; (b) *endo* isomer.

Table 2 Relative Energy (kcal/mol) and Dihedrals (degrees) of the AMBER and *ab initio* Minima Characterized for the Norbornane Dipeptides Represented in Figure 4

	AMBER			RHF/6-31G*		
	E(kcal/mol)	$\phi$	$\psi$	E(kcal/mol)	$\phi$	$\psi$
<i>exo</i>						
A	0.51	-64	67	0	-77	66
B	0	65	-64	0.57	77	-72
D	7.87	144	-170	6.46	154	-146
<i>endo</i>						
A	0	-62	70	0	-76	62
B	0.62	62	-79	1.03	73	-80
C	1.95	55	14	1.94	67	36
D	9.19	145	-161	6.29	158	-142
E	11.21	-131	-169	(a)		
F	9.68	-61	173	9.00	-66	-172

<sup>a</sup> Minimization leads to minimum F.

All these conformational features can be explained on the grounds of the steric interactions between the bicycle skeleton and the amino and carboxyl substituents. Furthermore, given that the *exo* or *endo* position occupied by these substituents is the only difference between the two compounds, it must account for their distinct conformational properties.

As shown schematically in Figure 6, a substituent in *endo* introduces a much higher steric hindrance than when it is substituted in *exo*. Both the *exo* and *endo* moieties at C $\alpha$  are eclipsed with one of the  $\beta$  hydrogens (H $_{3x}$  and H $_{3n}$ , respectively) but, whereas the former lies next to one of the hydrogens of the methylene bridge (H $_7$ ), the *endo* substituent is located in close proximity to the two *endo*-disposed hydrogens of the ethylene unit (H $_5$ , H $_6$ ).

Moreover, the different steric requirements of each substituent should be taken into account. The closest van der Waals contacts between the norbornane skeleton and the amino and carboxyl termini occur at high absolute  $\phi$  and  $\psi$  values and involve mainly the acetyl oxygen atom of the acetamino group (-NHC(=O)Me) and the amide hydrogen of the methylcarboxamide moiety (-CONHMe), as illustrated in Figure 7a,c. Because of the larger volume of the oxygen atom and the longer distance of the C=O bond in comparison to N-H, for a given *exo/endo* stereochemistry the acetamido group introduces a larger steric hindrance than does the carboxyl substituent. In comparison, the steric interactions

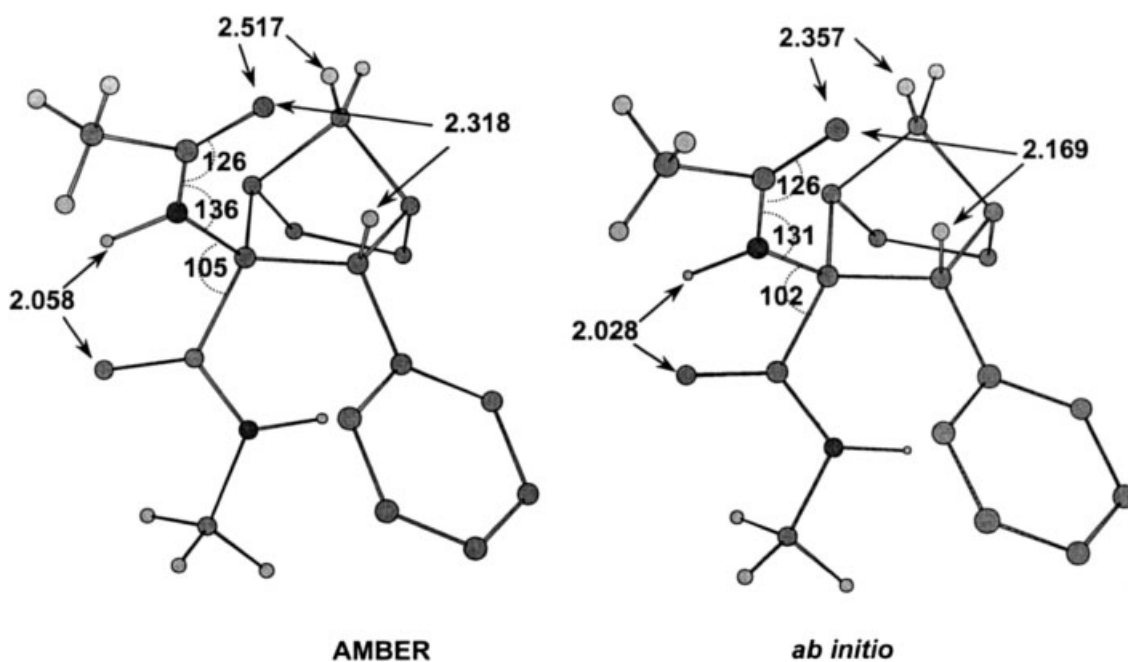


Figure 5 Structures of minimum **D** characterized for the *trans-endo* norbornane analogue of L-phenylalanine by molecular (left) and quantum (right) mechanics calculations. Energies and dihedral angles are given in Table 1.

bicycle/substituents for low absolute values of  $\phi$  and  $\psi$  are negligible (Figure 7b,d) with one exception: when the carboxamide substituent occupies an *endo* position, the oxygen atom ( $-\text{CONHMe}$ ) is involved in a repulsive interaction with a bicycle hydrogen, which is maximal at  $\psi$  around  $-30^\circ$  (Figure 7d).

The steric interactions considered above modulate the conformational features of the maps shown in Figure 4. The *exo* norbornane amino acid exhibits the amino moiety in an *endo* position. According to the previous considerations, this situation should be reflected in a strong restriction on the  $\phi$  torsion, as in fact is observed in Figure 4a. High values of  $\phi$ , either positive or negative, are very disfavoured due to the close proximity between the acetyl oxygen and three bicycle hydrogens. Figure 7a shows the

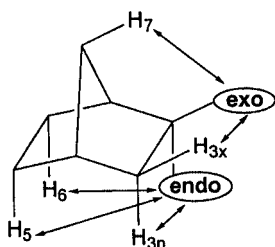


Figure 6 Steric interactions between the norbornane skeleton and a substituent occupying an *exo* or an *endo* position.

$\phi$  values at which these interactions are maximal. The closest contact occurs for  $\phi = -150^\circ$ , where  $\text{H}_6$  and the acetyl oxygen overlap, and gives rise to a high energy barrier on the map (Figure 4a). In comparison, the  $\psi$  dihedral is much less restricted, as expected for an *exo* carboxamide substituent. The most significant interactions that this group is involved in are those between the amide hydrogen and both hydrogens  $\text{H}_7$  and  $\text{H}_{3x}$ , and occur at values of  $\psi$  near  $170^\circ$  and  $-120^\circ$ , respectively (Figure 7a). For this reason valley **B** appears less extended than valley **A** at high values of  $\psi$ . In summary, the steric constraints imposed by the bicycle skeleton to the substituents provide a basis for understanding the features of the  $(\phi, \psi)$  map for the *exo* norbornane amino acid.

In the *endo* residue (Figure 4b) the carboxyl group occupies an *endo* position and, as a consequence, rotation about the  $\psi$  dihedral is much more restricted than in the *exo* isomer, whereas the opposite is observed for the  $\phi$  torsion associated with an *exo*-oriented amino moiety. In general, high  $\phi$  and  $\psi$  values are disfavoured, and the specific values at which steric interactions with the bicycle hydrogens are maximal are depicted diagrammatically in Figure 7c. A weaker restriction on  $\phi$  accounts for the widening of valleys **A** and **B** on the map, providing a wider range of values for



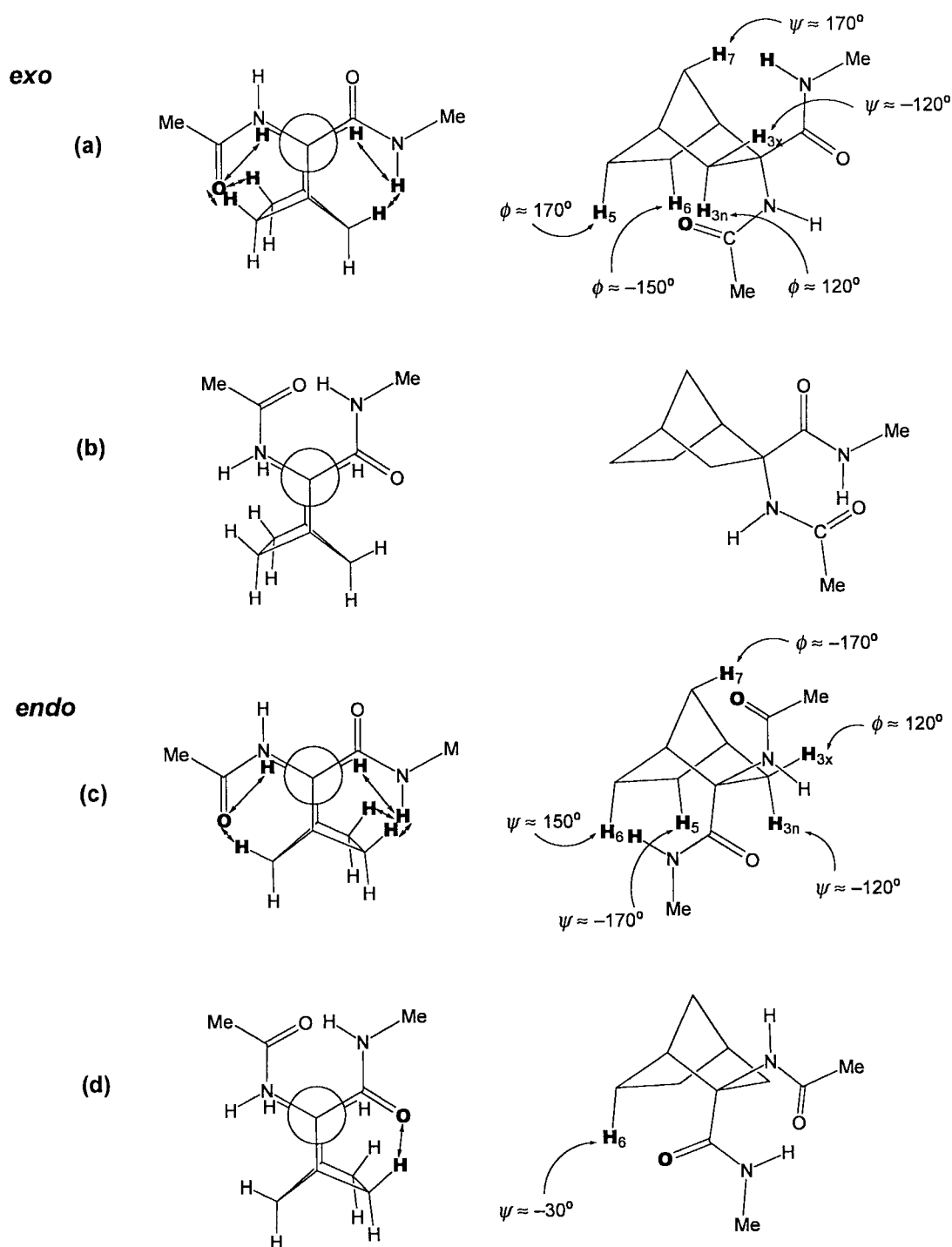


Figure 7 Newman projections through the  $C^\alpha-C^\beta$  bond of the *exo* and *endo* norbornane dipeptides represented in Figure 4, showing the steric interactions between the acetylamino and methylcarboxamide substituents and the bicycle (the atoms involved are indicated in bold characters). For each residue, two projections, corresponding to different dispositions of the substituents, are given. The  $\phi$ ,  $\psi$  values leading to the closest van der Waals contacts are indicated on the right (the bicycle hydrogens not involved in repulsive interactions are omitted for clarity).

this dihedral. On the other hand, the energy barrier exhibited at  $\psi = 150^\circ$  is responsible for the less favourable energy environment of valley **A** towards higher values of  $\psi$  compared with its *exo* isomer shown in Figure 4a. Another remarkable difference seen in Figure 4b is the splitting of the axial C7 conformation into two minima, due to the repulsive van der Waals contacts between the *endo* -CONHMe oxygen and the H<sub>6</sub> hydrogen for values of  $\psi$  close to  $-30^\circ$  (Figure 7d). In order to alleviate this steric hindrance, the  $\psi$  dihedral adopts higher or lower values than in the *exo* isomer, giving rise to two minima (**B** and **C**, Figure 4b; at  $\psi = -80^\circ$  and  $15^\circ$ , respectively). In minimum **C**, the intramolecular hydrogen bond is disrupted and, as a result, it exhibits a higher relative energy.

The conformational properties of the unsubstituted norbornane amino acids (Figure 4) constitute the basis for understanding the features observed in the Ramachandran plots of the norbornane analogues of L-phenylalanine shown in Figure 3. As can be seen, the aromatic side chain affects the mobility of the acetylamino and carboxamide substituents to a different extent for each stereoisomer. For steric reasons the phenyl ring is required to be in a relative eclipsed position, and as a consequence the  $\chi^1$  dihedral, that is determined by the configuration at C $^\alpha$  and C $^\beta$ , is confined to adopt values  $\chi^1 \approx 0^\circ$  in the case of the *cis* compounds, and  $\chi^1 \approx 120^\circ$  for the *trans* derivatives. This has a great impact on the

values accessible to  $\phi$  and  $\psi$  as can be seen from the comparison of the maps shown in Figures 3 and 4. These constraining effects are more pronounced on  $\phi$ , because the oxygen-to-aromatic ring distance of the repulsive interaction experienced by the phenyl group with the -NHCOMe and -CONHMe oxygen atoms is much shorter in the former case (Figure 8).

The bulky phenyl group not only limits the conformational mobility of the substituent that occupies a *cis* relative disposition, but also interacts sterically with the norbornane skeleton. In an attempt to minimize this steric hindrance, the bicyclic structure adopts a distorted geometry and this is reflected by  $\chi^1$  values that deviate from those expected for a regular norbornane system (Table 1).

Furthermore, as already mentioned, the steric strain produced by a bulky substituent is especially noticeable in the *endo* orientation. In the case of an *endo* phenyl substituent, the interactions with the bicycle skeleton affect the orientation of the phenyl plane (defined by the  $\chi^2$  dihedral angle). Although in phenylalanine torsion around  $\chi^2$  is not constrained, computational calculations suggest a marked preference to adopt values in the  $\pm 90^\circ$  region [22,28]. This orientation of the phenyl plane that minimizes unfavourable contacts with the main chain, is also predominantly accommodated by aromatic residues in the crystal structure of proteins [29]. Values of  $\chi^2$  near  $90^\circ$  have also been encountered in the crystalline structure of

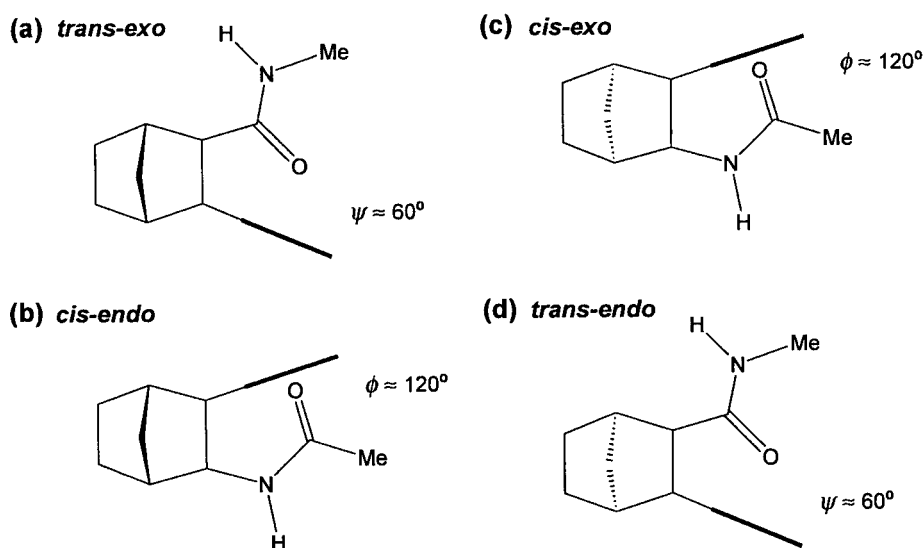


Figure 8 Repulsive interactions between the aromatic ring and the amino or carboxyl substituent occupying a *cis* relative position for each of the phenylnorbornane dipeptides represented in Figure 3. The  $\phi$  or  $\psi$  value leading to the closest oxygen/phenyl proximity is indicated in each case. The phenyl ring, in a plane perpendicular to the paper, is represented by a thick line.

peptides containing  $c_3\text{Phe}$  and  $c_6\text{Phe}$  [13,15]. In the phenylalanine norbornane surrogates with an *exo*-oriented phenyl side chain,  $90^\circ$  is a value accessible to  $\chi^2$  and, in fact, most of the minima characterized for these residues exhibit  $\chi^2$  dihedrals that deviate little from it (Table 1). However, when the phenyl ring occupies an *endo* position, the  $\chi^2$  dihedral cannot attain the  $90^\circ$  region, since it leads to the overlapping of an *ortho* aromatic hydrogen with an *endo* hydrogen of the bicycle (Figure 9). As a consequence, the  $\chi^2$  angle is forced to assume values either in the  $50^\circ$ – $60^\circ$  or in the  $120^\circ$ – $130^\circ$  region (Table 1). These restrictions on  $\chi^2$  may, in turn, modify the  $(\phi, \psi)$  space because deviations of  $\chi^2$  from the  $90^\circ$  region increase the interactions between the phenyl ring and the amino and carboxyl substituents.

The effects associated with the presence of the phenyl side chain provide clues to understanding the differences between the conformational profiles of the phenylnorbornane amino acids (Figure 3) and their parent norbornane residues (Figure 4).

The Ramachandran map of the *trans-exo*  $\text{L}$ -phenylalanine norbornane analogue is represented in Figure 3a. The high restriction experienced by the  $\phi$  torsion in the unsubstituted *exo* compound,

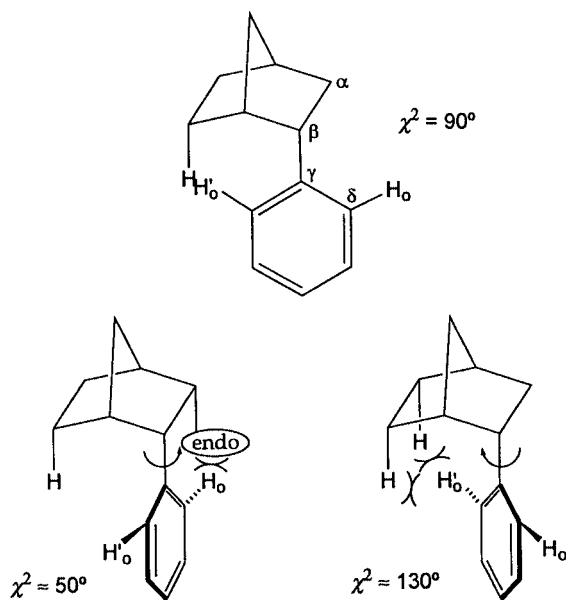


Figure 9 Overlapping of a bicycle hydrogen with an *ortho* aromatic hydrogen produced at  $\chi^2 = 90^\circ$  when the phenyl ring occupies an *endo* position in the phenylnorbornane dipeptides studied (top). Values accessible to  $\chi^2$  for an *endo* phenyl substituent, showing the steric interactions originated (bottom). The  $\chi^2$  angle is defined by  $C^\alpha - C^\beta - C^\gamma - C^\delta$ .

with intense energy barriers centred at  $120^\circ$ ,  $170^\circ$  and  $-150^\circ$  (Figures 4a and 7a), is maintained because the aromatic moiety has little effect on the torsion of the acetamino group. In contrast, rotation about the  $C^\alpha - C'$  angle, which is relatively free in the absence of the phenyl ring, is much more limited in Figure 3a. For positive  $\psi$  values, the oxygen atom of the  $-\text{CONHMe}$  group lies close to the eclipsed phenyl ring and, accordingly, a significant increase in the relative energy of the upper half of the map ( $\psi > 0^\circ$ ) is observed. The proximity O/phenyl, and therefore the destabilizing interaction originated, becomes maximal at  $\psi \approx 60^\circ$  (Figure 8a). As a result, valley **A** in Figure 4a, centred at  $\psi = 67^\circ$  and characterized by a small energy variation along the  $\psi$  axis, splits into two minima that appear at  $\psi$  values around  $150^\circ$  and  $0^\circ$  (Figure 3a, minima **A** and **C**, respectively). In minimum **C**, a deviation of the  $\chi^2$  angle to  $117^\circ$  contributes to alleviating the O/phenyl repulsion. The secondary minimum **D**, corresponding to an extended C5 structure, is maintained because it does not present any special interaction with the aromatic moiety. Thus, at variance with the behaviour shown by the *exo* parent residue, the *trans-exo* phenylnorbornane amino acid exhibits a clear preference for the C7 axial region of the conformational map, (minimum B) that in addition, exhibits a more constrained  $\psi$  component than its parent compound, due to the phenyl ring.

The *cis-endo* phenylnorbornane isomer also bears the aromatic side chain in an *exo* position but, in this case, the acetamido group is eclipsed. Its Ramachandran map (Figure 3b) is very similar to that of the unsubstituted *endo* residue (Figure 4b), although a considerable increase in energy of the right-hand side of the map ( $\phi > 0^\circ$ ) is observed. The comparison of the two maps suggests that whereas the  $\psi$  dihedral is not affected by the aromatic substituent, a dramatic restriction on the rotation about the  $C^\alpha - \text{N}$  angle is produced. Positive values of  $\phi$  place the acetyl oxygen atom in close proximity to the aromatic ring, especially for  $\phi = 120^\circ$  (Figure 8b). The repulsion produced displaces minima **B** and **C** to lower  $\phi$  values ( $\approx 45^\circ$ , Table 1) than those found for the unsubstituted *endo* amino acid ( $\approx 60^\circ$ , Table 2). Thus, whereas in Figure 4b the two C7 conformations exhibit similar energies, in the *cis-endo*  $\text{L}$ -phenylalanine norbornane analogue, the equatorial C7 structure is much lower energy than any other region on the map.

In the *cis-exo* phenylnorbornane analogue (Figure 3c) the aromatic ring and the acetamido

group are also in a *cis* relative disposition. The direct influence exerted by the phenyl substituent on the  $\phi$  torsion is, therefore, identical to that described in the previous paragraph for the *cis-endo* isomer, i.e. a considerable increase in energy of the right-hand side of the map, particularly in the  $\phi = 120^\circ$  region, as a result of the phenyl/acetyl oxygen repulsive interaction (Figure 8c). However, in the case of the *cis-exo* compound, both the phenyl and acetamido groups occupy an *endo* position producing a larger steric hindrance with the norbornane structure. Constraints on the  $\phi$  torsion, already very high in the absence of the phenyl ring (Figure 4a), attain an extreme level in Figure 3c, and only the  $\phi = -60^\circ$  region remains accessible. The appearance of several minima in this low-energy region of the map (**A**, **C** and **F**, Figure 3c) can be related to the restriction associated with the  $\chi^2$  dihedral when the phenyl side chain adopts an *endo* orientation (Figure 9). At stated above,  $\chi^2$  is forced to assume values around  $50^\circ$  or  $120^\circ$  and, in the  $\phi = -60^\circ$  region, both of them prove compatible with a  $\psi$  angle near  $70^\circ$  (Table 1). Two regular C7 structures differing on  $\chi^2$  (**A**, **F**) are therefore characterized as minima both at the molecular and at the quantum mechanics level, with **F** being slightly disfavoured because the position corresponding to the phenyl plane for  $\chi^2 = 120^\circ$  introduces a larger steric interaction with the bicycle (Figure 9). For the more favourable  $\chi^2$  value of  $50^\circ$ , AMBER locates an additional minimum at a lower  $\psi$  angle (**C**) than in the *ab initio* computations leading to the optimal  $70^\circ$  value.

The higher complexity observed in the right-hand side of the map in Figure 3c with respect to that of its parent residue (Figure 4a) can also be related to the restriction on the  $\chi^2$  torsion. In this region ( $\phi \approx 50^\circ$ ), when  $\chi^2$  deviates towards  $120^\circ$ ,  $\psi$  can assume the value corresponding to an ideal C7 conformation (minimum **B**,  $\psi \approx -70^\circ$ ), but this is not feasible for  $\chi^2$  near  $60^\circ$  (minimum **E**,  $\psi \approx 0^\circ$ ) since it would lead to a close contact between an *ortho* aromatic hydrogen and the -CONHMe amide hydrogen. The less favourable geometry for intramolecular hydrogen-bonding in minimum **E** seems to compensate for the higher steric hindrance phenyl/bicycle associated with the  $\chi^2$  angle in minimum **B**, and both minima exhibit similar energies. However, they are very destabilized with respect to the minima in the  $\phi = -60^\circ$  region, as is the extended conformation (minimum **D**).

The conformational properties exhibited by the *cis-exo* phenylnorbornane residue are the result of an extremely restricted  $\phi$  dihedral and a relatively

free rotation of the  $\psi$  torsion. The opposite situation is found for the *trans-endo* isomer (Figure 3d): whereas no high energy barriers are associated with the  $\phi$  torsion, the mobility of the *endo* carboxamide substituent is firstly restricted by interactions with the norbornane skeleton (as shown for the unsubstituted *endo* residue in Figures 4b and 7c,d), and additionally by the introduction of a phenyl group in a *cis* relative disposition (as explained for the *trans-exo* phenylnorbornane amino acid). The extremely high restriction on  $\psi$ , together with that on  $\chi^2$  associated with an *endo* phenyl substituent, gives rise to an enormous complexity in the conformational profile of the *trans-endo* phenylnorbornane amino acid (Figure 3d). The global minimum corresponds to an axial C7 structure, due to the destabilization induced by the phenyl moiety at positive  $\psi$  angles. Moreover, the intense energy barrier encountered at  $\psi = 60^\circ$  and originated by the high proximity between the -CONHMe oxygen and the aromatic ring (Figure 8d) results in the splitting of the equatorial C7 minimum, as described in the case of the *trans-exo* residue. The secondary minima **D** and **E** maintain the positions found for the unsubstituted *endo* amino acid, suggesting that the phenyl group does not introduce additional constraints for extended conformations with negative  $\psi$  values. Some extra minima, arising from the influence of the constrained  $\chi^2$  values on the  $(\phi, \psi)$  preferences, are also present. The complexity of the map shown in Figure 3d, together with the discrepancies shown by AMBER and *ab initio* in the description of the stability and geometry of some minima (mainly of minimum **D**, as already discussed) make it difficult to establish with certainty their relative stability and, thereafter, to predict the conformational behaviour of the *trans-endo* phenylnorbornane amino acid.

## CONCLUSIONS

The conformational profile of the four possible stereoisomeric L-phenylalanine norbornane analogues has been assessed by computational methods. Ramachandran maps were computed at the molecular mechanics level using the parm94 parameterization of the AMBER force field. Low-energy conformations were also computed at the *ab initio* level. The results show only small discrepancies between the two methods that are due to the overestimation of the repulsion energy between the acetyl

oxygen and the bicycle skeleton in the molecular mechanics calculations.

The main conformational features of the norbornane analogues of L-phenylalanine can be explained in terms of the constraining effects exerted by both the bicycle skeleton and the aromatic moiety on the space available to the peptide backbone. Due to steric interactions with the amino and carboxyl substituents, the norbornane skeleton hampers extended conformations in favour of folded C7-like structures. However, the bicycle itself does not induce a significant energy difference between the two C7 conformations. The symmetry is broken by the phenyl ring that is confined to an almost eclipsed orientation and introduces a strong destabilization of the right-hand side of the Ramachandran map ( $\phi > 0^\circ$ ) for the *cis* derivatives and of the upper half ( $\psi > 0^\circ$ ) for the *trans* isomers.

Independently of the geometric and energetic details of the different relative low-energy conformations found, the most interesting aspect of the present results is the fact that the conformational space of the phenylnorbornane amino acids investigated (and that of their four enantiomers) is severely constrained. Taking as a measure of this constraint the proportion of the ( $\phi, \psi$ ) space under an arbitrary threshold of 5 kcal/mol above the global minimum, these residues exhibit only about 6%–8%, in comparison to the 15%–20% found for standard amino acids. In the case of the *trans-endo* isomer this proportion is probably underestimated, if we take into consideration the discrepancies between the molecular mechanics and the *ab initio* calculations.

The results suggest that the low-energy space available to each stereoisomer (with the exception of the *trans-endo* derivative) is restricted to only a region of the Ramachandran map. Additionally, the rigidity of the bicycle confines the  $\chi^1$  angle to a very narrow range, and in the *endo* derivatives the  $\chi^2$  space is restricted for steric reasons. All these characteristics contribute to make the norbornane analogues of phenylalanine interesting candidates in the design of constrained peptides, particularly in those studies aimed at evaluating the influence of side chain restriction on structure and activity.

### Acknowledgements

The authors wish to express their gratitude to CESCO and CEPBA for a generous allocation of computer time through a grant-in-aid to the project Molecular Engineering. Financial support from

DGES (PM98-0012-C02-01 and PPQ2001-1834) is gratefully acknowledged.

### REFERENCES

1. McDowell RS, Artis DR. Structure-based design from flexible ligands. *Annu. Rep. Med. Chem.* 1995; **30**: 265–274.
2. Balaram P. Non-standard amino acids in peptide design and protein engineering. *Curr. Opin. Struct. Biol.* 1992; **2**: 845–851.
3. Rizo J, Gierasch LM. Constrained peptides: models of bioactive peptides and protein substructures. *Annu. Rev. Biochem.* 1992; **61**: 387–418.
4. Hanessian S, McNaughtonSmith G, Lombart HG, Lubell WD. Design and synthesis of conformationally constrained amino acids as versatile scaffolds and peptide mimetics. *Tetrahedron* 1997; **53**: 12 789–12 854.
5. Hruba VJ. Design in topographical space of peptide and peptidomimetic ligands that affect behavior. A chemist's glimpse at the mind-body problem. *Acc. Chem. Res.* 2001; **34**: 389–397.
6. Marshall GR. Three-dimensional structure of peptide–protein complexes: implications for recognition. *Curr. Opin. Struct. Biol.* 1992; **2**: 904–919.
7. Perutz MF. The role of aromatic rings as hydrogen-bond acceptors in molecular recognition. *Philos. Trans. R. Soc.* 1993; **A345**: 105–112.
8. McGaughey GB, Gagne M, Rappe AK.  $\pi$ -Stacking interactions. *J. Biol. Chem.* 1998; **273**: 15 458–15 463.
9. Burley SK, Petsko GA. Amino-aromatic interactions in proteins. *FEBS Lett.* 1986; **203**: 139–143.
10. Nishio M, Hirota M, Umezawa Y. *The CH/ $\pi$  Interaction: Evidence, Nature and Consequences*. John Wiley & Sons: New York, 1998.
11. Gomez-Catalan J, Perez JJ, Jimenez AI, Cativiela C. Study of the conformational profile of selected unnatural amino acid residues derived from L-phenylalanine. *J. Peptide Sci.* 1999; **5**: 251–262.
12. Gomez-Catalan J, Jimenez AI, Cativiela C, Perez JJ. Study of the conformational profile of the cyclohexane analogs of L-phenylalanine. *J. Peptide Res.* 2001; **57**: 435–446.
13. Jimenez AI, Cativiela C, Gomez-Catalan J, Perez JJ, Aubry A, Paris M, Marraud M. Influence of side chain restriction and NH... $\pi$  interaction on the  $\beta$ -turn folding modes of dipeptides incorporating phenylalanine cyclohexane derivatives. *J. Am. Chem. Soc.* 2000; **122**: 5811–5821.
14. Jimenez AI, Cativiela C, Paris M, Peregrina JM, Avenoza A, Aubry A, Marraud M.  $\beta$ -Turn modulation by the cyclohexane analogues of phenylalanine. *Tetrahedron Lett.* 1998; **39**: 7841–7844.

15. Jimenez AI, Vanderesse R, Marraud M, Aubry A, Cativiela C.  $\beta$ -Turn preferences induced by 2,3-methanophenylalanine chirality. *J. Am. Chem. Soc.* 1998; **120**: 9452–9459.
16. Jimenez AI, Vanderesse R, Marraud M, Aubry A, Cativiela C. Folding types of dipeptides containing the diastereoisomeric cyclopropanic analogs of phenylalanine. *Tetrahedron Lett.* 1997; **38**: 7559–7562.
17. Christensen HN, Handlogten ME, Lam I, Tager HS, Zand R. A bicyclic amino acid to improve discriminations among transport systems. *J. Biol. Chem.* 1969; **244**: 1510–1520.
18. Van Winkle LJ, Christensen HN, Campione AL. Na<sup>+</sup>-dependent transport of basic, zwitterionic, and bicyclic amino acids by a broad-scope system in mouse blastocysts. *J. Biol. Chem.* 1985; **260**: 12 118–12 123.
19. Avenzoza A, Cativiela C, Mayoral JA, Roy MA. Synthesis of the four DL-pairs of 2-amino-3-phenylnorbornane-2-carboxylic acids. *Tetrahedron* 1989; **45**: 3923–3934.
20. Cativiela C, Mayoral JA, Avenzoza A, González M, Roy MA. 5(4H)-Oxazolones as dienophiles in the synthesis of 2-amino-2-bicycloalkanecarboxylic acids. *Synthesis* 1990; 1114–1116.
21. Cativiela C, Díaz-de-Villegas MD, Mayoral JA, Avenzoza A, Peregrina JM. Synthesis of the four D,L-pairs of 2-amino-3-phenylnorbornane-2-carboxylic acids II. The use of 5(4H)-oxazolones as dienophiles. *Tetrahedron* 1993; **49**: 677–684.
22. Hruby VJ, Li G, Haskell-Luevano C, Shenderovich M. Design of peptides, proteins and peptidomimetics in chi space. *Biopolymers* 1997; **43**: 219–266.
23. Cornell WD, Cieplak P, Bayly CL, Gould IR, Merz KM, Ferguson DM, Spellmeyer DC, Fox T, Caldwell JW, Kollman PA. A second generation force field for the simulation of proteins, nucleic acids and organic molecules. *J. Am. Chem. Soc.* 1995; **117**: 5179–5197.
24. Frisch MJ, Trucks GW, Schlegel HB, Gill PMW, Johnson BG, Robb MA, Cheeseman JR, Keith T, Peterson GA, Montgomery JA, Raghavachari K, Al-Laham MA, Zakrzewski VG, Ortiz JV, Foresman JB, Peng CY, Ayala PY, Chen W, Wong MW, Andres JL, Replogle ES, Gomperts R, Martin RL, Fox J, Binkley JS, Defrees DJ, Baker J, Stewart JJP, Head-Gordon M, Gonzales C, Pople JA. *Gaussian94, Revision B.2.* Gaussian Inc: Pittsburgh PA, 1995.
25. Head-Gordon T, Head-Gordon M, Frisch MJ, Brooks III CL, Pople JA. Theoretical study of blocked glycine and alanine peptide analogues. *J. Am. Chem. Soc.* 1991; **113**: 5989–5997.
26. Bohm HJ, Brode S. *Ab initio* SCF calculations on low-energy conformers of *N*-acetyl-*N'*-methylalaninamide and *N*-acetyl-*N'*-methylglycinamide. *J. Am. Chem. Soc.* 1991; **113**: 7129–7135.
27. Gould IR, Cornell WD, Hillier IH. A quantum mechanical investigation of the conformational energetics of the alanine and glycine dipeptides in the gas phase and in aqueous solution. *J. Am. Chem. Soc.* 1994; **116**: 9250–9256.
28. Jáklí I, Perczel A, Farkas O, Hollosi M, Csizmadia IG. Peptide models XXII. A conformational model for aromatic amino acid residues in proteins. A comprehensive analysis of all the RHF/6-31 + G\* conformers of For-L-Phe-NH<sub>2</sub>. *J. Mol. Struct. (Theochem)* 1998; **455**: 303–314.
29. Gould RO, Gray AM, Taylor P, Walkinshaw MD. Crystal environments and geometries of leucine, isoleucine, valine, and phenylalanine provide estimates of minimum nonbonded contact and preferred van der Waals interaction distances. *J. Am. Chem. Soc.* 1985; **107**: 5921–5927.